

## Hydrogen site occupancies in single-walled carbon nanotubes studied by inelastic neutron scattering

This article has been downloaded from IOPscience. Please scroll down to see the full text article.

2004 J. Phys.: Condens. Matter 16 L73

(<http://iopscience.iop.org/0953-8984/16/8/L01>)

View [the table of contents for this issue](#), or go to the [journal homepage](#) for more

Download details:

IP Address: 129.252.86.83

The article was downloaded on 27/05/2010 at 12:44

Please note that [terms and conditions apply](#).

## LETTER TO THE EDITOR

## Hydrogen site occupancies in single-walled carbon nanotubes studied by inelastic neutron scattering

P A Georgiev<sup>1</sup>, D K Ross<sup>1</sup>, A De Monte<sup>2</sup>, U Montaretto-Marullo<sup>2</sup>,  
R A H Edwards<sup>2</sup>, A J Ramirez-Cuesta<sup>3</sup> and D Colognesi<sup>3,4</sup>

<sup>1</sup> Institute for Materials Research, University of Salford, Salford M5 4WT, UK

<sup>2</sup> Institute for Renewable Energy, J R C Ispra (VA) 21020, Italy

<sup>3</sup> ISIS Facility, Rutherford Appleton Laboratory, Chilton, Didcot, Oxon, UK

Received 3 November 2003

Published 13 February 2004

Online at [stacks.iop.org/JPhysCM/16/L73](http://stacks.iop.org/JPhysCM/16/L73) (DOI: 10.1088/0953-8984/16/8/L01)

### Abstract

Neutron inelastic scattering spectra from high quality single-wall carbon nanotubes (SWNTs), progressively dosed with hydrogen, have been measured with high resolution at different temperatures in the vicinity of 20 K. The spectra consist of two parts. Firstly, a relatively sharp complex peak, due to scattering from translationally bound molecules undergoing rotational transitions, is observed at around 14.5 meV. Secondly, there is a series of broad features at higher energies originating from roto-vibrational transitions corresponding to  $J = 0$  to 1 rotational change plus  $n = 0$  to  $n = 1, 2$ , etc molecular centre-of-mass vibrational transitions, as well as from molecule centre-of-mass recoil. The structure of the complex sharp peak suggests that the molecular hydrogen is adsorbed on at least two different adsorption sites on the surfaces of the nanotube bundles.

It is generally recognized that, to compete with hydrocarbon fuels, a hydrogen storage system should reversibly store at least 7% by weight of hydrogen. Single-walled carbon nanotubes (SWNTs) became of interest in this context because of published claims of very large hydrogen storage capacity at ambient temperatures [1–3]. Although these claims have since been refuted [4, 5], there remains a serious interest in the use of SWNTs for hydrogen storage at liquid nitrogen temperatures through physisorption, due to the large external surface area/gram available and the possibility that the hydrogen could be stored inside the tubes. However, in spite of numerous publications on the subject, there is as yet no consensus as to where and how the hydrogen is being adsorbed. In this letter, we report on the use of inelastic neutron scattering, combined with progressive *in situ* surface dosing, to probe the nature of this hydrogen adsorption process. Earlier, lower resolution, measurements [6, 7] showed the scattering to be dominated by physisorbed molecular hydrogen. However, due to the

<sup>4</sup> Present address: CNR—Istituto di Fisica Applicata, ‘N Carrara’, Firenze, Italy.

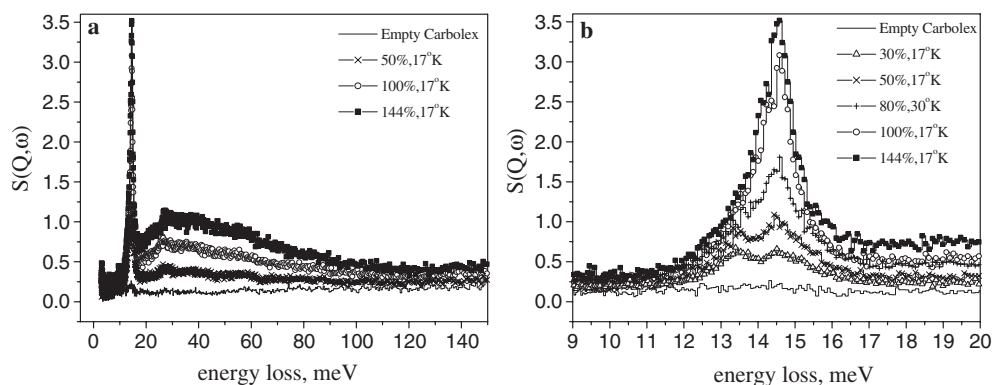


**Figure 1.** (a) Inelastic neutron spectra of SWNTs loaded with different amounts of  $p$ -H<sub>2</sub> as indicated in the figure legend. The increase of the hydrogen content is best seen in the intensity increase of the first recoil peak at about 30 meV corresponding to an internal transition from  $J = 0$  to 1. (b) The bound part of the spectra at different  $p$ -H<sub>2</sub> contents around the first rotational transition. From the bottom to the top, spectra with increasing hydrogen loadings are shown. Some of the spectra measured have been omitted here for clarity.

insufficient instrument resolution available in those investigations, the details of the rotational transitions were not measured and, in consequence, the effects of different site geometries could not be observed. A Raman scattering study [8] of the molecular spectra of hydrogen isotopes adsorbed in SWNTs showed shifts in the  $Q$  branch (vibrational 0–1 level), which the authors attribute to Lennard-Jones potentials and image forces in conducting SWNTs, and hence they conclude that there is no charge transfer between the H<sub>2</sub> and the SWNTs. The present neutron scattering measurements have been made on the TOSCA spectrometer at ISIS (Rutherford Appleton Laboratory, UK) in neutron energy loss as a function of surface loading, which, in turn, has been fully calibrated against gravimetric uptake measurements. The resolution of TOSCA in this energy transfer range is about 0.3 meV. The sample used was non-purified selected grade SWNT material from CarboLex Inc., as used in [7]. It consists of ropes of SWNTs of diameter about 1.5 nm. Gas adsorption isotherms for both hydrogen and nitrogen were measured at 77 K using an IGA instrument [9]. Typical type II N<sub>2</sub> adsorption and fully reversible desorption isotherms were observed up to the saturation pressure, yielding the specific surface area from the BET (Brunauer, Emmet and Teller) equation, and also indicating that there is no accessible micro-porosity. The derived surface area was 371 m<sup>2</sup> g<sup>-1</sup> compared to the calculated 1315 m<sup>2</sup> g<sup>-1</sup>, for one side of a graphene sheet. We assume, therefore, that the observed adsorption takes place on the exterior of the nanotube ropes, in any large voids formed between different ropes and/or at defects in the close packed rope bundle. From the isotherm, we cannot rule out the penetration of the nanotubes by a small proportion of the H<sub>2</sub> molecules. A total of 1.1 wt% of hydrogen uptake was measured at 10 bar and 77 K.

The aim of our neutron measurement was to probe the structure of the rotational energy spectrum of the adsorbate molecules at different adsorption sites by measuring the spectra as a function of H<sub>2</sub> loading. In the absence of significant external interactions, hydrogen behaves as a perfect quantum rotor with energy levels given by  $E_J = B_J J(J + 1)$  where  $B_J = 7.35$  meV [10] is the rotational constant and  $J$  is the rotational quantum number. The symmetry of the total wavefunction implies that *para*-hydrogen (proton spins anti-parallel) only exists in even  $J$  states while *ortho*-hydrogen (proton spins parallel) only exists for odd  $J$ , for which the lowest energy level is 14.7 meV. In the neutron energy loss regime, the highest

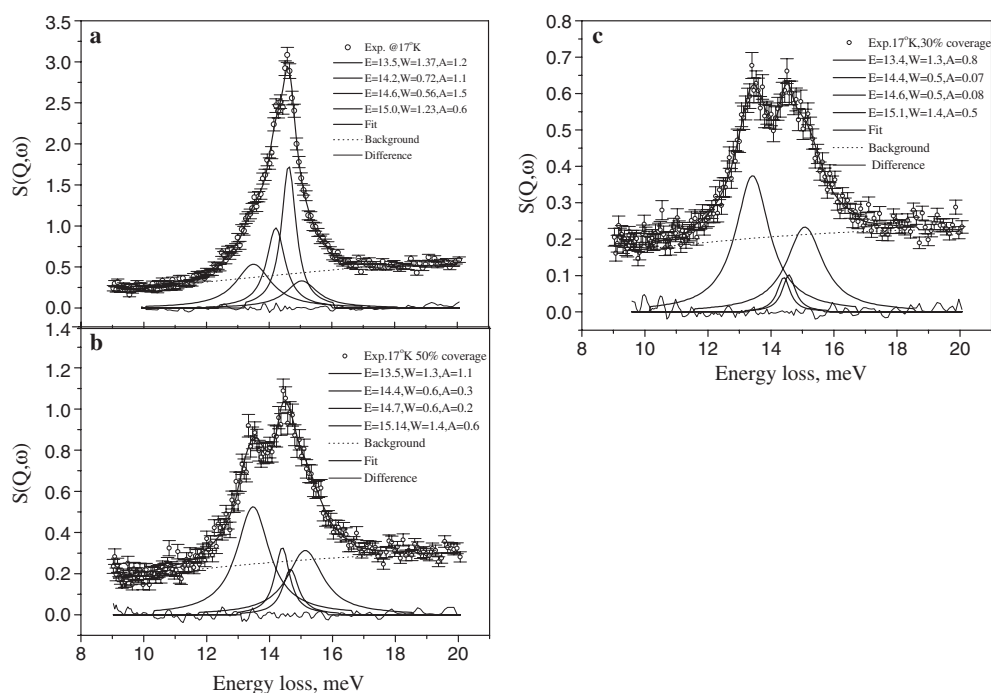


**Figure 2.** (a) The bound part of the scattering collected from a complete monolayer of  $p$ -H<sub>2</sub> at 17 K fitted with four Lorentzians, (b) the fitted spectrum measured with 50% coverage at 17 K, (c) 30% average surface coverage and 17 K.  $E$  is the peak position in meV,  $W$  is the full width at the half maximum in meV and  $A$  is the relative peak area. The split rotational line is significantly broadened presumably due to the presence of a range of barriers to rotation.

scattering cross section occurs for the  $J = 0$  to 1 transition [11] and this determined our strategy. We used a series of different loadings of  $p$ -H<sub>2</sub>, prepared at 20 K by storing the gas over a paramagnetic catalyst for 48 h, and made our measurements at a number of temperatures in the vicinity of 20 K. Prior to the neutron measurements, the sample in its Al sample can was degassed at 150 °C for 48 h under a vacuum of around  $10^{-6}$  Torr. Some of the spectra collected are shown in figure 1, in the region of the  $J = 0$  to 1 transition. Spectra collected at 20 K and 100% coverage, and at 25 K with 85% coverage, are omitted for clarity. The temperature and surface coverage for each spectrum is given in the figure legends. The coverage was calculated assuming that the molecular area of the N<sub>2</sub> molecule at 77 K is  $16.2 \text{ \AA}^2$ , estimated from the density of the corresponding liquid state [12], whereas that of the H<sub>2</sub> at 20 K was assumed to be  $10.8 \text{ \AA}^2$ , as derived from the intermolecular distances densest incommensurate monolayer configuration of hydrogen on a graphitic surface [13]. The complex character of the peaks around 14.5 meV is revealed in figure 1(b). In figure 2, we show this part of the spectrum, measured for different surface coverages at 17 K and fitted with a series of four Lorentzians, with parameters given in the figure legends. The other spectra were analysed in the same fashion. In the fitting process, all the peak parameters were allowed to float, except at the highest coverage of 144%, where we had to fix the peak positions and widths to get a stable fit. With all parameters varying, fairly constant peak positions and widths were found for the different temperatures and surface coverages. The exception to this was the 14.2 meV line, the width of which increased substantially at 30 K, figure 3. A three-peak model was also tested on our data but this led to a 12% increase in  $\chi^2$ , and larger variation in the peak

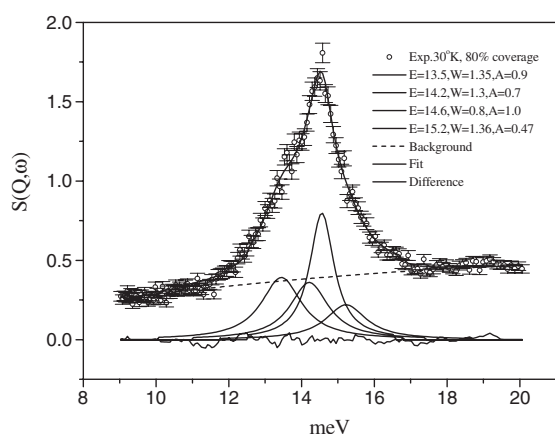


**Figure 3.** 30 K data measured from 80% surface coverage.

positions. Also, the three-peak model gave an intensity ratio of the 13.5 meV line to that of the 15.1 meV of around 3/1—compared to  $\sim 2/1$  for the four-peak model, a ratio that is much easier to explain. This makes us confident of the need to include four peaks in the fit. In contrast to the peak energies, the integrated intensities of each line vary in a distinct way with the surface coverage as indicated in figure 4. Here we note that the peaks at 13.5 and 15.1 meV first grow with increasing coverage and then saturate at around 50% surface coverage, having a constant statistical weight ratio of about 2/1. In contrast, the lines at 14.2 and 14.6 meV initially have a low intensity and then increase strongly, eventually saturating at a loading above monolayer coverage. The observed 2/1 intensity ratio of the 13.5 and 15.1 meV peaks—independent of temperature or loading—makes it reasonable to assume that these peaks arise from scattering from a ground *para*-state ( $J = 0$ ) to a ground *ortho*-state ( $J = 1$ ) where the threefold degeneracy of the latter state has been lifted by the shape of the potential at the adsorption site [14, 15] yielding two states with defined angular momentum component perpendicular to the surface ( $m = \pm 1$ ) and one with angular momentum parallel to the surface ( $m = 0$ ). The  $m = \pm 1$  states, in which the molecule rotates with  $\mathbf{J}$  normal to the surface, have lower energies than those with  $m = 0$ , where the molecule rotates with angular momentum vector in an undetermined direction parallel to the surface. Physically, this form of splitting would be expected at a planar graphite surface where the  $\text{H}_2$  molecule is attracted to the surface by a Lennard-Jones type potential. Thus, we would expect the  $m = \pm 1$  states to be lower in energy than the  $m = 0$  state because, in the former cases, the wavefunction is able to stay closer to the minimum of the potential energy curve normal to the surface. The split line, as defined above, has a centre of gravity of 14.0 meV whereas a first order perturbation effect should leave the mean energy unaltered. Here, we would note that the scattering from *para*-hydrogen interstitially adsorbed in the octahedral site in solid  $\text{C}_{60}$  shows a split peak with a centre of gravity at 14.4 meV [16]. In this letter, the shift in the mean energy is attributed to the existence of different zero-point energies associated with the different molecular vibrations at the different  $m$  values of the  $J = 1$  state and this effect could operate here as well. A downward shift of 0.7 meV has been observed for  $\text{H}_2$  adsorbed on Vycor glass [18]. A similar form of splitting, but with a somewhat larger magnitude of 2.6 meV, was recently predicted [17] for  $\text{H}_2$  molecules inside (10, 10) SWNTs.

The third of the fitted peaks, centred at 14.6 meV, is clearly due to the scattering of a rotationally free hydrogen from its ground state with  $J = 0$  via spin flip to the  $J = 1$  level, observed at 14.7 meV on flat graphite surfaces [19]. We would note from the variation in

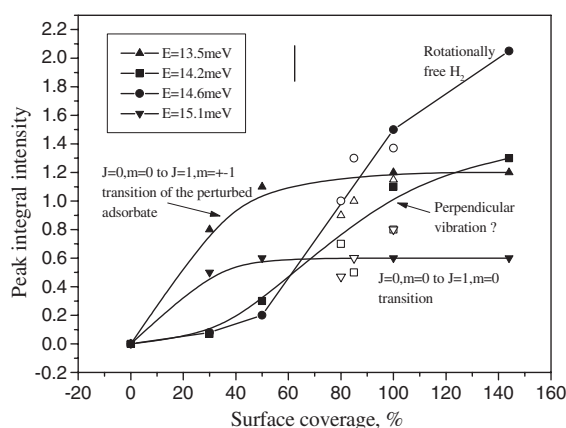


**Figure 4.** Integral peak intensities as a function of the average surface coverage. The curves connect points corresponding to data collected at 17 K and are only a guide to the eye. The corresponding open shapes are due to data measured at 20, 25 and 30 K. Thermally activated desorption is observed with increasing temperature except that the 14.2 meV line intensity increases between 25 and 30 K. The bar in the upper part of the figure indicates the average size of the error bars at different points.

the peak intensities in figure 4 that the 14.6 meV peak is filled last. This suggests that this peak is indeed due to more weakly bound molecules, perhaps adsorbed on the external convex surface of the tubes or in a second molecular layer. Note that, at the finite  $Q$  values of these measurements ( $4 \text{ \AA}^{-1}$ ), the intensities do not exactly correspond to the populations on the different sites because the trapping potential affects the Debye–Waller factor. This leaves the peak at 14.2 meV. Its intensity variation with coverage implies that it has an intermediate adsorption energy. We would suggest that this is either due to a  $J = 0$  to 1 transition for molecules trapped on a third site on or in the nanotubes or to the vibration of the hydrogen molecules in the potential well normal to the graphitic surface. The difficulty with the first hypothesis is that this energy shift corresponds to a 1.5% increase in the H–H distance and this would imply charge transfer to the substrate corresponding to a significant increase in the binding energy of the site, contrary to the implications of the variation of intensity with surface coverage. Further, experimental studies [8] and simulations [20] suggest that no charge transfer occurs on adsorption and that the relaxed inter-nuclear distance of the  $\text{H}_2$  molecule,  $0.741 \text{ \AA}$ , is the same as in the free rotor.

On the other hand, we would note that a vibrational peak has been observed at this energy for  $o\text{-H}_2$ <sup>1</sup> in  $\text{C}_{60}$  [16]. Moreover, experimental observations [21] and model calculations [22] of adsorbed hydrogen on a planar graphite sheet suggest an out-of-plane vibrational transition from the ground to the first excited state at 15.0 and 14.3 meV respectively. Also, the small feature at 28–29 meV in figure 1(a) can be attributed to a coupled  $J = 0$  to 1 rotational plus an  $n = 0$  to 1 excitation of a vibration normal to the planar surface.

On the other hand, the cross section for a vibrational centre-of-mass excitation, corresponding to a transition within the  $J = 0$  manifold ( $p\text{-H}_2$ ), is only a few per cent of that for the *para-ortho* [11]. A possible explanation for this unexpectedly large intensity might be that the strong coupling between the rotational and vibrational modes of similar energies would break down the distinction between the pure *ortho*- and pure *para*-states and hence would modify the ratio of the two cross sections. Finally, we would note that the intensity

<sup>1</sup> In this case, transitions within the  $J = 1$  manifold are expected to show the highest intensity [11].

of this peak increased by about 25% when the temperature increased from 25 to 30 K. This is not unexpected because of the approximately 2% increase in the *ortho*-component of the adsorbed gas going from 25 to 30 K and the strong  $J_1$ - $J_1$  cross section [11]. However, we cannot definitely distinguish between these possibilities at present.

We should also point out that the widths of our measured lines are not resolution limited, the instrument resolution at these energies being of the order of 0.3 meV. The split rotational transition shows the largest broadening, possibly due to variation in the shape of the potential well on the surface. All levels can also be broadened via damping through acoustic phonons in the substrate.

Thus, from our measurements, we can conclude that the adsorbed molecular hydrogen is distributed over at least two energetically different adsorption sites on the external surface of the nanotube bundle and possibly in voids formed between bundles or in defects within the tube bundles. A preferred adsorption site is presumably the valley between two adjacent tubes. This would imply some azimuthal barrier to rotation giving either splitting or broadening but we must assume that these effects are too small to be observed in the presence of other broadening effects. Molecules on the external convex tube surface are free to rotate and to recoil parallel to the surface. When the capacity of these two types of site is exceeded, the extra hydrogen forms normal multi-layer condensate which is free to rotate and to recoil. We have thus shown that inelastic neutron scattering from samples progressively dosed with hydrogen provides a powerful method of analysing the sorption mechanisms involved.

The authors are pleased to thank the ISIS staff for providing the neutrons and the instrumentation, and particularly John Dreyer and Chris Goodway for the help with the gas handling rigs.

## References

- [1] Dillon A C, Jones K M, Bekkedahl T A, Bethune D S and Heben M J 1997 *Nature* **386** 377–9
- [2] Chambers A, Park C, Baker R T K and Rodriguez N M 1998 *J. Phys. Chem. B* **102** 4253–6
- [3] Chen P, Wu X, Lin J and Tan K L 1999 *Science* **285** 91–3
- [4] Yang R T 2000 *Carbon* **38** 623–31
- [5] Ye Y, Ahn C C, Witham C, Fultz B, Liu J, Rinzler G, Colbert D, Smith K A and Smalley R E 1999 *Appl. Phys. Lett.* **74** 2307–9
- [6] Brown C M, Yildirim T, Neumann D A, Heben M J, Gennet T, Dillon A C, Alleman J L and Fischer J E 2000 *Chem. Phys. Lett.* **329** 311–6
- [7] Ren Y and Price D L 2001 *Appl. Phys. Lett.* **79** 3684–6
- [8] Williams K A, Pradhan K B, Eklund P C, Kostov M K and Cole M W 2002 *Phys. Rev. Lett.* **88** 165502
- [9] <http://www.hidenisochema.com/>
- [10] Stoicheff B P 1957 *Can. J. Phys.* **35** 730
- [11] Young J A and Koppel J U 1964 *Phys. Rev. A* **135** 603–11
- [12] Gregg S J and Sing K S W 1982 *Adsorption Surface Area and Porosity* (London: Academic)
- [13] Freimuth H, Wiechert H and Lauter H J 1987 *Surf. Sci.* **189/190** 548
- [14] Smith A P, Benedek R, Trouw F R, Minkoff M and Yang L H 1996 *Phys. Rev. B* **53** 10187
- [15] Ramirez-Cuesta A J, Mitchel P C H and Parker S F 2001 *J. Mol. Catal. A* **167** 217–24
- [16] FitzGerald S A, Yildirim T, Santodonato L J, Neumann D A, Copley J R D, Rush J J and Trow F 1991 *Phys. Rev. B* **60** 6439–51
- [17] Silvera I F and Nielsen M 1976 *Phys. Rev. Lett.* **37** 1275
- [18] Brown D W, Sokol P E and FitzGerald S A 1999 *Phys. Rev. B* **59** 13258
- [19] Yildirim T and Harris A B 2003 *Phys. Rev. B* **67** 245413
- [20] Arellano J S, Molina L M, Rubio A, Lopez M J and Alonso J A 2002 *J. Chem. Phys.* **117** 2281
- [21] Mattera L, Rosatelli F, Salvo C, Tommasini F, Valbusa U and Vidali G 1980 *Surf. Sci.* **93** 515
- [22] Crowell A D and Brown J S 1982 *Surf. Sci.* **123** 296